N95- 20520

RADIATION EFFECTS ON p+n InP JUNCTIONS GROWN BY MOCVD

S.R. Messenger
SFA, Inc.
Landover, Maryland

R.J. Walters
U.S. Naval Research Laboratory
Washington, DC

M.J. Panunto
University of Maryland Baltimore County
Baltimore, Maryland

and

G.P. Summers
U.S. Naval Research Laboratory
Washington, DC

INTRODUCTION

The superior radiation resistance of InP over other solar cell materials such as Si or GaAs has prompted the development of InP cells for space applications. The early research on radiation effects in InP was performed by Yamaguchi and co-workers who showed that, in diffused p-InP junctions, radiation-induced defects were readily annealed both thermally and by injection, which was accompanied by significant cell recovery.

More recent research efforts have been made using p-InP grown by metalorganic chemical vapor deposition (MOCVD). While similar deep level transient spectroscopy (DLTS) results were found for radiation induced defects in these cells and in diffused junctions, significant differences existed in the annealing characteristics. After injection annealing at room temperature, Yamaguchi noticed an almost complete recovery of the photovoltaic parameters, while the MOCVD samples showed only minimal annealing.

In searching for an explanation of the different annealing behavior of diffused junctions and those grown by MOCVD, several possibilities have been considered. One possibility is the difference in the emitter structure. The diffused junctions have S-doped graded emitters with widths of ~0.3μm,while the MOCVD emitters are often doped with Si and have widths of ~300Å (0.03μm). The difference in the emitter thickness can have important effects, e.g. a larger fraction of the total photocurrent is generated in the n-type material for thicker emitters. Therefore the properties of the n-InP material may explain the difference in the observed overall annealing behavior of the cells.

EXPERIMENTAL

In this study, n-InP solar cells and mesa diodes were irradiated with either 1 MeV electrons or 3 MeV protons, with both (current-voltage) IV and DLTS measurements being made. The IV measurements were performed both in the dark and under 1 sun AM0 illuminations using an Oriel 1000W portable Xe arc lamp simulator. A Kepco 50-2M bipolar amplifier, and two Keithley 617 electrometers were employed in the IV measurements, which were computer controlled through a GPIB interface. DLTS and capacitance-voltage (CV) measurements were performed using the Bio-Rad DL4600 system which uses the Boonton 72-B capacitance meter. The cryostat used in the DLTS system has a temperature range of 85-500K which allows annealing experiments to be performed directly in the cryostat. The cryostat window is made of sapphire which allows for cell illumination as well. All cell measurements were thus performed in the cryostat. This unique system provides a simple and convenient means for collecting cell data.

The samples were grown by Spire Corporation using Si as the n-type base dopant. Figure 1 gives a schematic description of the samples. The base dopant level was ~3 x 10^{16} cm^{-3} and that of the emitter was ~2 x 10^{18} cm^{-3}, both of which were determined from CV measurements.

1 MeV electron irradiations were performed at a Van de Graaff accelerator at the NASA Goddard Space Flight Center in Greenbelt, MD. Incremental fluences were performed up to ~10^{16}

e^-/cm^2. The beam currents were low enough (~150 nA) to avoid sample heating during the irradiations. Dosimetry is known to within 10-15%. The 3 MeV proton irradiations were performed at the Naval Surface Warfare Center in White Oak, MD on a Pelletron accelerator. One irradiation was performed giving a total fluence ~3 x 10^{12} p^+/cm^2 (15-20% accurate). The proton beam was rastered over a 2.4 cm^2 area, and the current on the target was ~14 nA/cm^2.

RESULTS

DLTS Measurements:

Figure 2 shows the DLTS spectrum measured on a p^+ n InP mesa diode after 1 MeV electron irradiation to a fluence ~10^{16} cm^{-3}. Majority carrier traps EN1-4, and EB are formed during the irradiation. One minority carrier trap, HN1, appears in small concentrations and seems to be due to a composite defect. The "EN" refers to electron trapping in n-type InP. Similarly, "HN" refers to hole trapping in n-InP. 3 MeV proton irradiation produces the same defect spectrum, except the relative peak heights are slightly different as shown in Figure 3. Trap EN1 is only seen using rate windows >1000/s. As can be seen in Figs. 2 and 3, EB is the dominant DLTS signal in both cases. The activation energy, capture cross section, and annealing characteristics of this peak are similar to those of the EB peak measured in irradiated p-type InP as shown by McKeever et al. in reference 1. No clear relationship between the remaining peaks and peaks measured in irradiated p-type InP seems to exist. The activation energy of the EN2 defect is similar to that of the ED defect measured in irradiated p-type InP (~0.3 eV) as seen in reference 2, but the capture cross section of EN2 is about two orders of magnitude larger than that of ED. Also, the activation energy of HN1 is similar to that of the H4 defect (0.34 eV at this dopant level) , but the capture cross section of HN1 is about an order of magnitude larger than that of H4. This may be due to the fact that HN1 is most likely several overlapping peaks. Tables I and II characterize each defect according to its activation energy, capture cross section, defect concentration, and introduction rate after 1 MeV electron and 3 MeV proton irradiations, respectively.

Introduction rates were calculated for the 1 MeV electron irradiations and are included in Table I. The errors are ~2-4%. Figure 4 shows DLTS data for the introduction of defects with 1 MeV electron irradiation. The calculated introduction rate for EB of 0.15 cm^{-1} is much lower than the value of 0.7 given for the dominant defect H4 in p-type InP by Sibille in reference 3 and also by Levinson et al. in reference 4 (who measured a value of 1.0). The total trap introduction rate is 0.2 cm^{-1} which is also much lower than that found for p-type InP as stated in references 3-5. The introduction rates for the 3 MeV protons were obtained from only one data point assuming a linear dependence. This is justified due to the linear relationships found in the 1 MeV electron irradiated samples. The total trap introduction rate here is 52.5 defects per incident proton per cm which compares nicely with the data shown by Walters and Summers in reference 6. Overall, there are much fewer stable defects created in n-type InP than there are in p-type InP. This same result was also seen by Levinson et al. in references 4 and 7.

Forward bias injection annealing at any temperature did not change the DLTS defect structure. This is in contrast to the behavior of the H4 defect in irradiated p-type InP which injection anneals readily at room temperature. Isochronal thermal annealing was performed on the electron irradiated junctions and the results are shown on Figure 5. It is seen that the only defect which thermal anneals is EB. By a temperature of ~400K, EB is completely removed. It should be mentioned that the annealing experiments were performed with the sample under a reverse bias of -2V. It was found that open circuit anneals led to an enhanced annealing rate. Experiments are currently under way dealing specifically with this effect. Thermal annealing both with and without an applied forward bias produces the same results implying that the annealing is not injection sensitive. There is therefore only one thermal annealing stage occurring ~360-380K (for the case of V_R =-2V) where the EB peak is completely removed. This happens to be the same temperature where EB anneals in p-type InP as

discussed in reference 1. Isothermal annealing experiments on EB indicate a thermal activation energy to be 1.23 ± 0.02 eV in a first order process. This is for the case of annealing with a bias voltage of -2V. For zero bias, the thermal activation energy is 1.13 eV. These thermal energies are close to the value of 1.02 eV that Yamaguchi measured in p-type diffused InP junctions for the H4 defect as shown in reference 8. Reference 9 contains isothermal annealing data on LEC n-InP material. The 0.79 eV defect there has annealing behavior which is very similar to that of EB. First of all, it is insensitive to injection just as shown above. Also, its thermal activation energy is 0.98 eV which is also close to what was measured above.

Illuminated IV Measurements:

Due to the similarity in the defect spectra under both electron and proton irradiation, the IV data were performed on the 3 MeV proton irradiated cells only. The first experiment measured the recovery of the cells due to illuminations below room temperature. The IV curves were taken at 86K because, in p-type InP, it has been found that illuminated IV measurements taken at 86K do not cause injection annealing (ref. 10). The annealing experiment consisted of measuring the illuminated IV curve at 86K before and after the 3 MeV proton irradiation. The cell was then warmed to 200K and illuminated, at short-circuit, for 35 minutes before being cooled to 86K where another illuminated IV measurement was made. This same procedure was performed for an illuminated anneal at 300K for 30 minutes. The measured IV curves are shown in Figure 6 and the photovoltaic (PV) parameters are given in Table III. The cell shows some recovery due to the illuminations. The largest increase is in the short circuit current (I_{sc}), but even this increase is small. The fill factor (FF) also increases slightly after the 200K illumination but not after the 300K illumination. The increase in these two parameters caused an increase in the maximum power (P_{max}), but the recovery is inhibited because the open circuit voltage (V_{oc}) shows no recovery. The next experiment was an anneal at room temperature. The same sample was then left in the dark at 300K for one week. As is seen in Figure 6, there is more recovery in I_{sc}, but it is again only slight.

The same cell was then illuminated above room temperature. In these experiments, the illuminated IV curves could be measured at room temperature without altering the results. Figure 7 includes the IV curves measured after 1 week in the dark to indicate the final state of the cell after the T≤300K annealing stages. The corresponding PV data is given in Table IV. Illuminating the cell at 350K for 4 hours caused significant recovery in all of the PV parameters. In particular, V_{oc} is seen to recover for the first time. Subsequently illuminating the cell at 400K for 3 hours caused increases in all of the parameters. Two hours of illumination at 450K only caused an increase in V_{oc}, but I_{sc} was unaffected.

The IV curve measured after the 450K illumination represents the maximum recovery of the cell. Significant recovery is evident, primarily due to the increase in I_{sc}. However, while the recovery is substantial, it is far from complete. In particular, almost none of the radiation-induced degradation of the FF has been removed. Also, V_{oc} shows only very little recovery.

Dark IV Measurements:

Measurements were also made of the dark IV characteristics. By fitting the measured dark IV data to the standard three-term diode equation, estimates of the diffusion term (I_{01}), the recombination term (I_{02}), and the shunt resistance term (R_{sh}) were determined. A commercially available curve fitting package, Peakfit, by Jandel Scientific was used. These fits were performed after each annealing step.

The forward bias dark current characteristics of the same cell used above were measured at room temperature before and after irradiation, as well as after the successive annealing treatments

described above. The measured data were fit to the following equation :

$$I(V) = I_{01}\left(e^{\frac{qV}{kT}} - 1\right) + I_{02}\left(e^{\frac{qV}{2kT}} - 1\right) + \frac{V}{R_{sh}}$$

where I_{01}, I_{02}, and R_{sh} are the diffusion, recombination, and shunt resistance fitting terms, respectively. In this equation, it was assumed that the energy level (E_t) of the dominant recombination center is located at the intrinsic Fermi Level (E_i). Attempts were made to fit the data with E_t as a free parameter, but the pre-irradiation recombination current in this particular cell was large enough that changes in E_t from E_i had virtually no effect on the fit. Some examples of the fits obtained are shown in Figure 8. The data for the fitting parameters are given in Table V for the annealing steps above. The fit to the pre-irradiation data does not seem to be very good. The reason for this is not known. Nevertheless, the fits to the post-irradiation and post-anneal data were excellent.

DISCUSSION

These results with p⁺n InP grown by MOCVD will now be compared with those obtained using n⁺p InP fabricated both by thermal diffusion and by MOCVD. The last SPRAT conference contains the data for the diffused junctions from reference 11. Figure 9 shows annealing data for all three of these cell types for the maximum power output. The scales are normalized to beginning-of-life (BOL). As seen on Fig. 9 the diffused junctions fully recover after a thermal anneal of 450K while both MOCVD cells do not recover even at 500K. Moreover, the slow recovery of both MOCVD cell types appears to be the same indicating similar behavior for n- and p-type InP. This trend is also apparent in Figure 10 where the same cell types are plotted this time for the normalized open circuit voltage. The fitted dark IV parameters I_{01} and I_{02} also follow this trend as can be seen on Figure 11. Figure 11 plots the data from Table V on scales normalized to BOL. The same slow recovery mentioned above occurs. It was also noticed at the last SPRAT conference from reference 12 that the radiation induced defects in p-InP did not anneal until thermal anneals at 650K were performed. It might the case that the PV parameters also would anneal at such temperatures, but the experiments have not been performed successfully.

CONCLUSION

Defect introduction and annealing studies were performed on Spire-grown n⁺p InP solar cells and mesa diodes. The introduction rates of the defects formed were shown to be much lower than the p-type counterparts. The annealing characteristics were, however, the same. In comparing the MOCVD samples with the diffused junctions, the diffused junctions showed much better annealing characteristics. Full recovery of the PV parameters existed in the diffused junctions where only minimal recovery is seen in the MOCVD samples. Future studies will try to explain this important difference.

REFERENCES

1. McKeever, S.W.S.; Walters, R.J.; Messenger, S.R.; and Summers, G.P.: Deep Level transient spectroscopy of irradiated p-type InP grown by metalorganic chemical vapor deposition. J. Appl. Phys., vol. 69, 1991, pp. 1435-1439.

2. Walters, R.J.; Messenger, S.R.; Summers, G.P.; Burke, E.A.; and Keavney, C.J.: Proton and electron irradiation of MOCVD InP solar cells: Experimental results and radiation modelling. Proc. of the 22nd IEEE Photovoltaic Specialists Conference, October 7-11, 1991, Las Vegas, NE, pp.1560-1565.

3. Sibille, A. and Bourgoin, J.C.: Electron irradiation induced deep levels in p-InP. Appl. Phys. Lett., vol. 41, 1982, pp. 956-958.

4. Levinson, M.; Temkin, H.; and Bonner, W.A.: Electron bombardment induced defect states in p-InP. J. Electron. Mater., vol. 12, 1983, pp.423-432.

5. Drevinsky, P.J.; Caefer, C.E.; and Keavney, C.J.: Processing- and radiation-produced defects in InP solar cells. Proc. of the 3rd IEEE International Conference on Indium Phosphide and Related Materials, Cardiff, Wales, April 8-11, 1991, pp. 56-59.

6. Walters, R.J. and Summers, G.P.: Deep level transient spectroscopy study of proton irradiated p-type InP. J. Appl. Phys., vol. 69, 1991, pp. 6488-6494.

7. Levinson, M.; Benton, J.L.; Temkin, H.; and Kimerling, L.C.: Defect states in electron bombarded n- InP. Appl. Phys. Lett., vol. 40, 1982, pp. 990-992.

8. Yamaguchi, M.; Ando, K.; Yamamoto, A.; and Uemura, C.: Injection-enhanced annealing of InP solar-cell radiation damage. J. Appl Phys., vol. 58, 1985, pp. 568-574.

9. Koyama, J.; Shirafuji, J.; and Inuishi, Y.: Annealing behaviour of gamma-ray-induced electron traps in LEC n-InP. Electronics Letters, vol. 19, 1983, pp.609-10.

10. Walters, R.J.:A study of the annealing of radiation-induced defects in InP solar cells. Doctoral dissertation, University of Maryland Baltimore County, May, 1994.

11. Walters, R.J.; Summers, G.P.; and Bruening, J.: A detailed study of the photo-injection annealing of thermally diffused InP solar cells. Proc. of the 12th Space Photovoltaic Research and Technology Conference, NASA Lewis, Oct. 20-22, 1992, pp. 1-7.

12. Messenger, S.R.; Walters, R.J.; and Summers, G.P.: High temperature annealing of the minority carrier traps in irradiated MOCVD n+p InP solar cell junctions. Same as ref. 11, pp. 8-15.

Table I DLTS defect parameters for 1 MeV electron irradiated n-InP diodes. The concentrations shown are for a 1 MeV electron fluence of 10^{16} cm^{-2} and a DLTS rate window of 2 s^{-1}.

Trap	Activation energy (eV)	Capture cross section (x 10^{-13} cm^2)	Concentration (x 10^{14} cm^{-3})	Introduction rate (cm^{-1})
EN2	0.31	2.05	0.1	-
EN3	0.48	2.37	1.3	0.013
EN4	0.55	0.287	1.8	0.018
EB	0.76	15.6	14.5	0.22

Table II DLTS defect parameters for 3 MeV proton irradiated n-InP. The fluence was 3 x 10^{12} cm^{-2}. The introduction rates were calculated assuming a linear dependence. The concentrations are for a rate window of 2/s.

Trap	Activation energy (eV)	Capture cross section (x $10^{-13}cm^2$)	Concentration (x $10^{13}cm^{-3}$)	Introduction rate (cm^{-1})
EN2	0.3	6.3	0.95	3.2
EN3	0.43	9.5	3.2	11
EN4	0.62	131	1.	4.7
EB	0.74	5	8.6	29
HN1	0.34	1.69	1.6	5.3

Table III Recovery of PV parameters of n-InP solar cell under short circuit illuminations from 200K to 400K. IV curves measured at 86K. Irradiation was 3 x 10^{12} 3 MeV protons cm^{-2}.

Condition	I_{sc} (mA)	V_{oc} (V)	P_{max} (mW)	FF	Eff(%)
Pre rad	21.88	1.270	29.90	0.9323	18.95
Post rad	17.71	1.229	17.82	0.8186	13.03
200K, 35 min.	17.84	1.231	18.12	0.8257	13.26
300K, 30 min.	18.03	1.230	18.29	0.8245	13.38
300K, 1 wk.	18.52	1.230	18.75	0.8230	13.71
350K, 4 hr.	18.58	1.231	18.74	0.8192	13.71
400K, 1 hr.	18.76	1.230	19.14	0.8293	14.00
400K, 3hr.	18.99	1.239	19.44	0.8259	14.22

Table IV Cell recovery under illumination from 300K to 450K. IV curves measured at 298K. Irradiation was 3 x 10^{12} 3 MeV protons cm^{-2}. "Post rad" data was taken after 35 min. illum. at 200K.

Condition	I_{sc} (mA)	V_{oc} (V)	P_{max} (mW)	FF	Eff(%)
Pre rad	25.13	0.8549	18.22	0.8480	13.33
Post rad	19.55	0.7633	11.21	0.7513	8.201
300K, 30 min.	19.58	0.7645	11.28	0.7537	8.251
300K, 1 wk.	20.03	0.7654	11.54	0.7528	8.443
350K, 15 min.	20.57	0.7662	11.87	0.7533	8.682
350K, 4 hr.	21.17	0.7731	12.40	0.7573	9.068
400K, 1 hr.	21.43	0.7761	12.61	0.7583	9.223
400K, 3 hr.	21.79	0.7806	12.95	0.7614	9.475
450K, 2 hr.	21.86	0.7875	13.10	0.7609	9.580

Table V Effect of illumination on the dark current parameters on n-InP solar cells irradiated with 3 MeV protons to a fluence of 3×10^{12} cm^{-2}. Parameters are from fits of the dark IV data.

Condition	I_{01} (x 10^{-16} A/cm^2)	I_{02} (x 10^{-9} A/cm^2)	R_{sh} (x 10^5 Ω)
Pre rad	1.099	0.1717	4.390
Post rad	9.451	3.090	3.665
350K, 15 min.	8.645	3.057	3.452
350K, 1.75 hr.	8.507	2.736	3.149
350K, 4 hr.	7.229	2.766	2.678
400K, 3 hr.	6.906	2.370	2.998
450K, 2 hr.	5.603	2.205	3.385

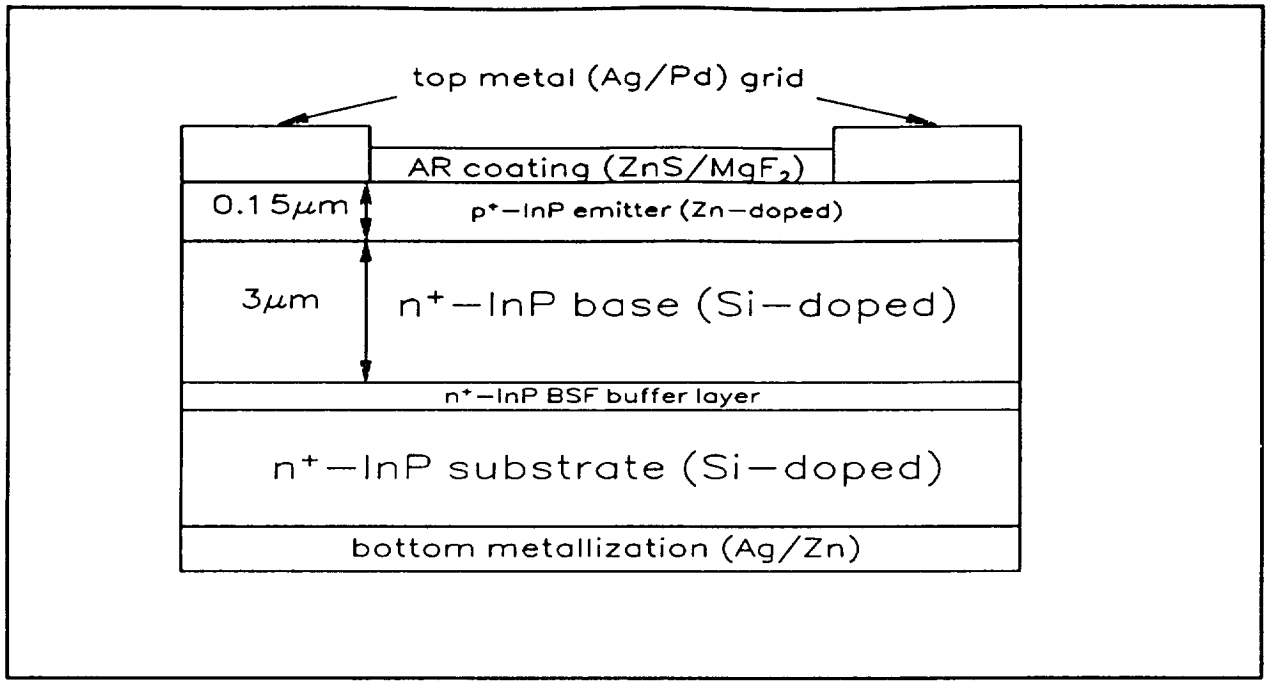

Figure 1 A schematic drawing of the p⁺n InP/InP cells.

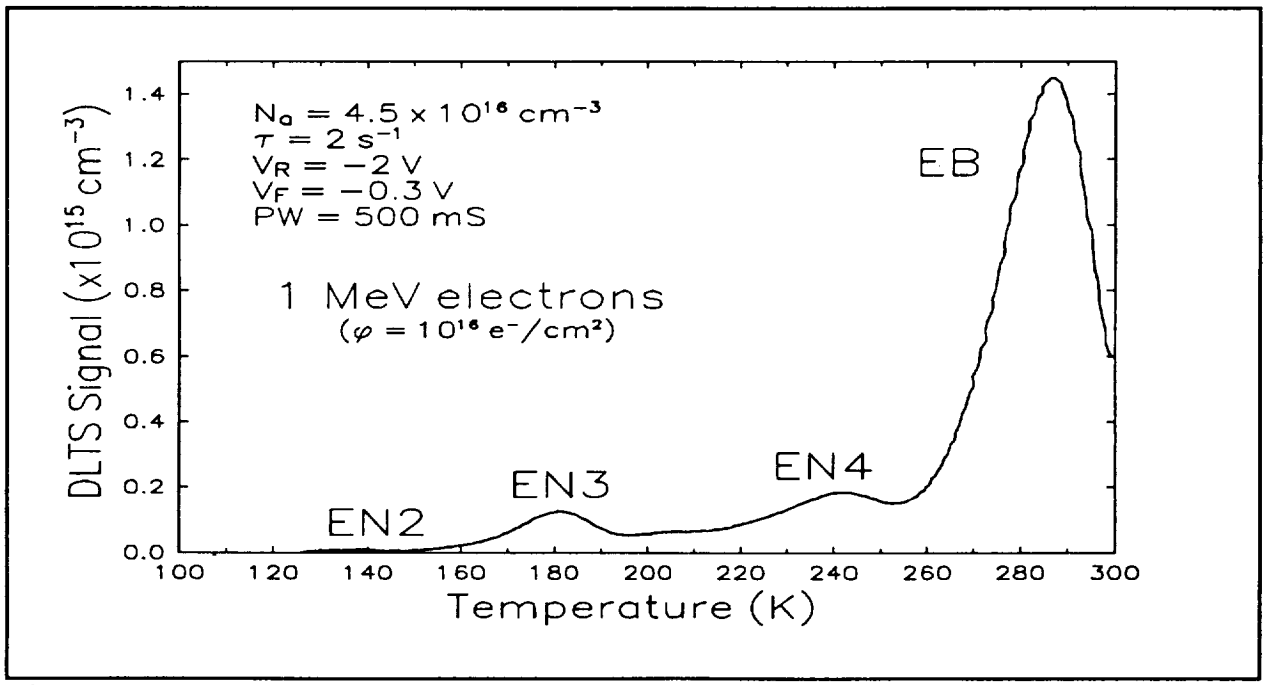

Figure 2 DLTS spectrum obtained after 1 MeV electron irradiation to a fluence of 1E16 cm^{-2}. The dominant peak, EB, is identified with the EB peak found in irradiated p-type InP.

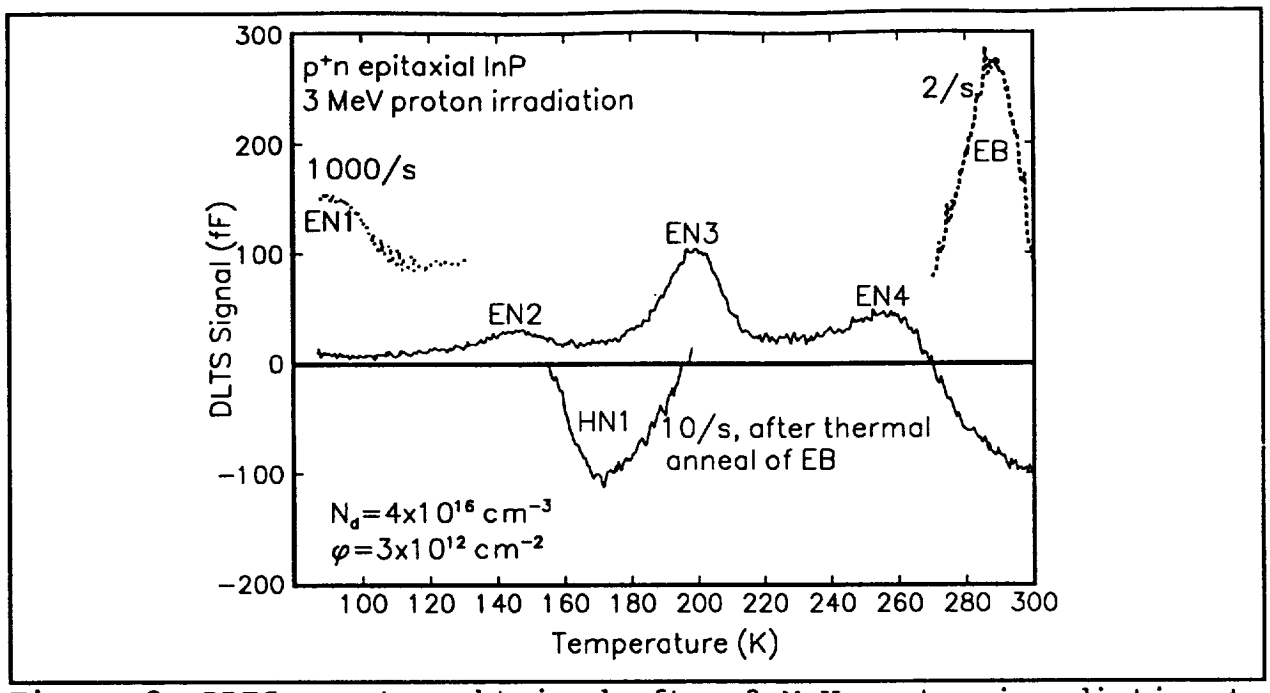

Figure 3 DLTS spectra obtained after 3 MeV proton irradiation to a fluence of $3x10^{12}$ cm^{-2}. The HN1 peak is most likely two overlapping peaks.

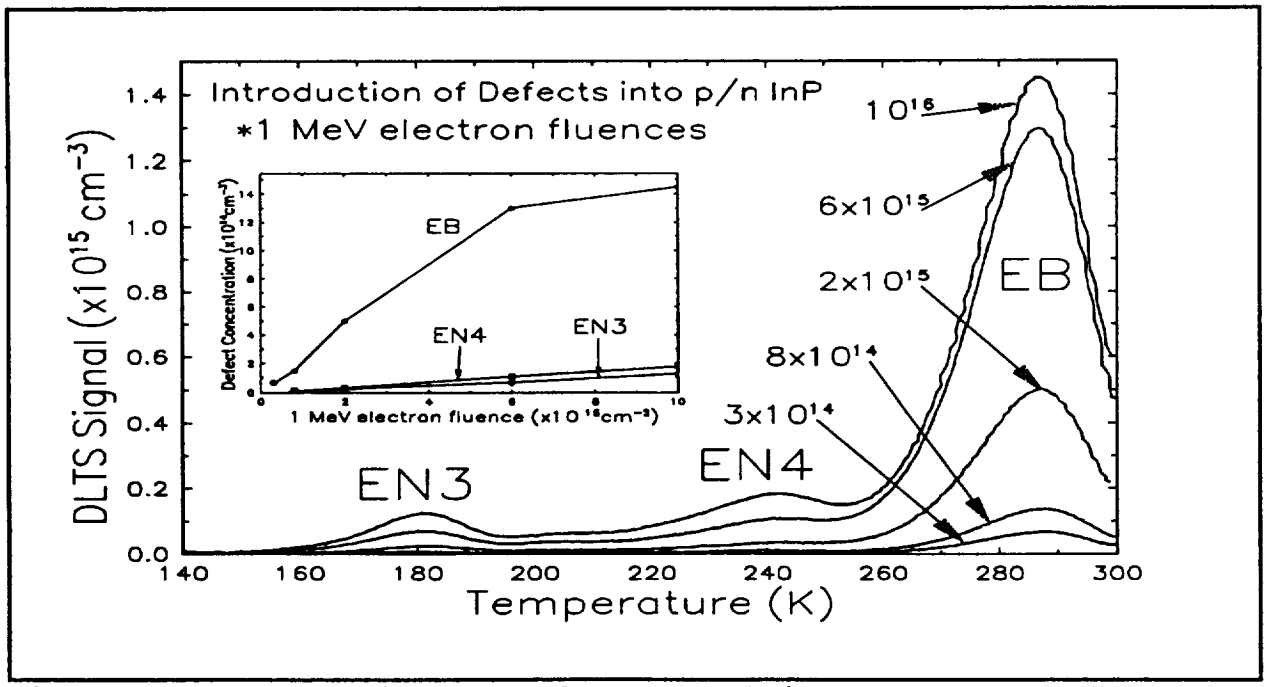

Figure 4 Introduction of defects resulting from 1 MeV electron irradiation. A linear dependence is found for all defects as shown in the inset.

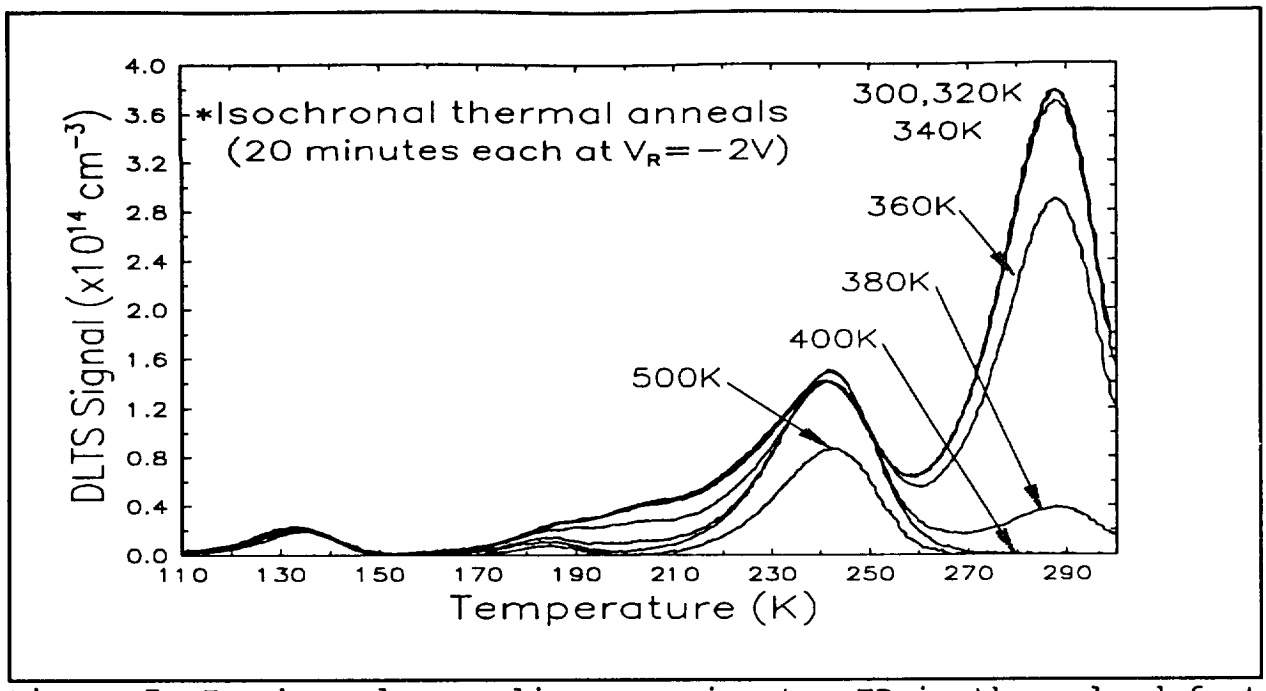

Figure 5 Isochronal annealing experiment. EB is the only defect which anneals. Holding the sample at V_R=-2V during the anneals, the annealing stage occurs ~380K.

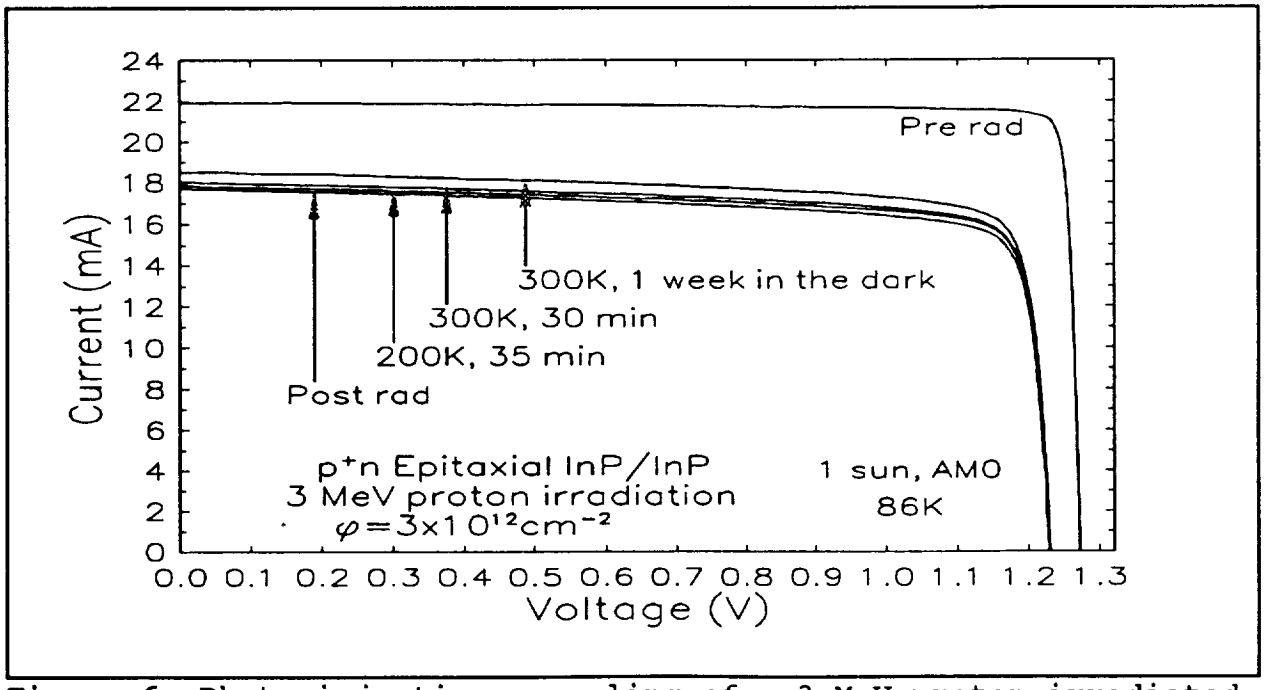

Figure 6 Photo-injection annealing of a 3 MeV proton irradiated n-InP cell. Illuminating the cell short circuited at 200K and then 300K caused a small increase in Isc and FF, but Voc did not change. The IV curves were taken at 86K.

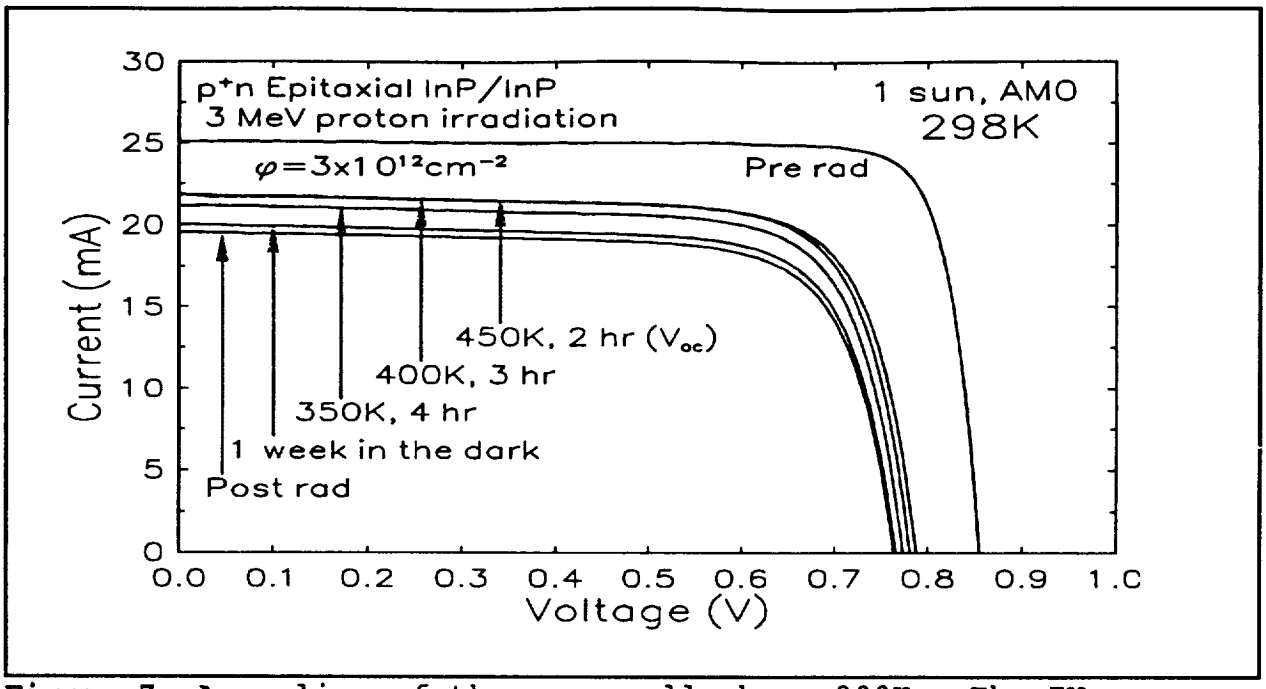

Figure 7 Annealing of the same cell above 300K. The IV curves were measured at 298K. All parameters recovered under illumination at 350K and 400K, but only Voc showed more recovery at 450K.

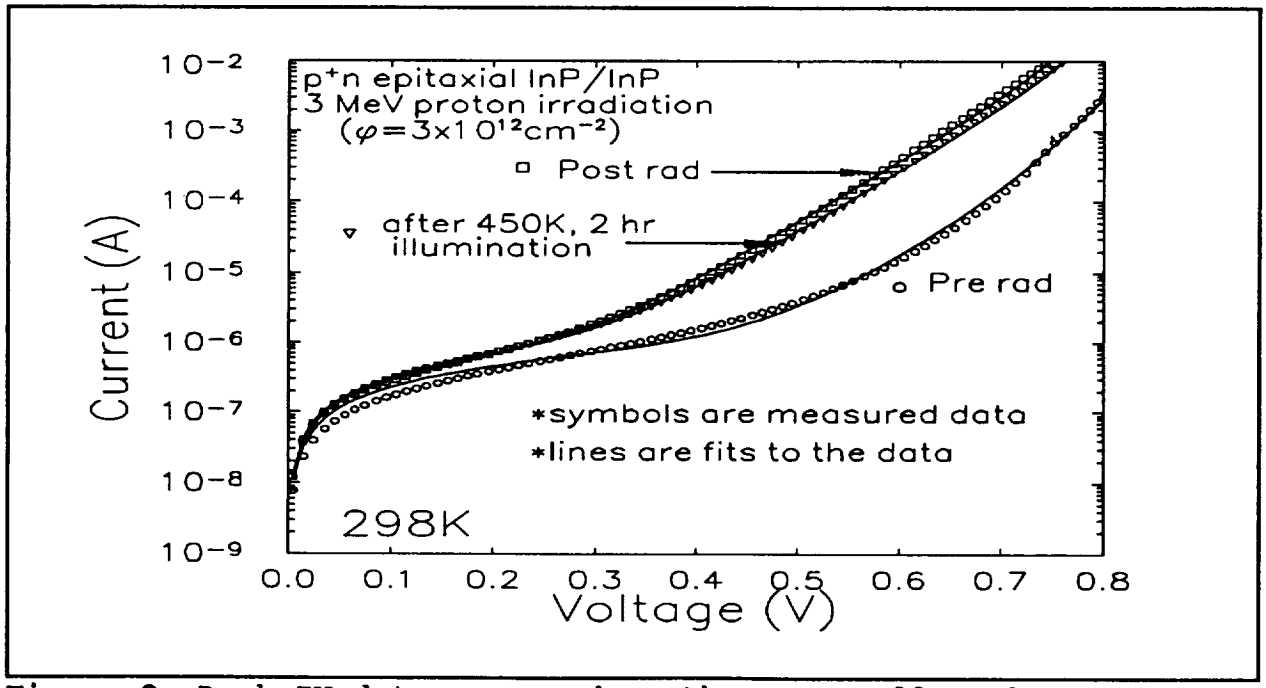

Figure 8 Dark IV data measured on the same cell. The irradiation increased both the recombination and generation currents, and the annealing caused only a small reduction.

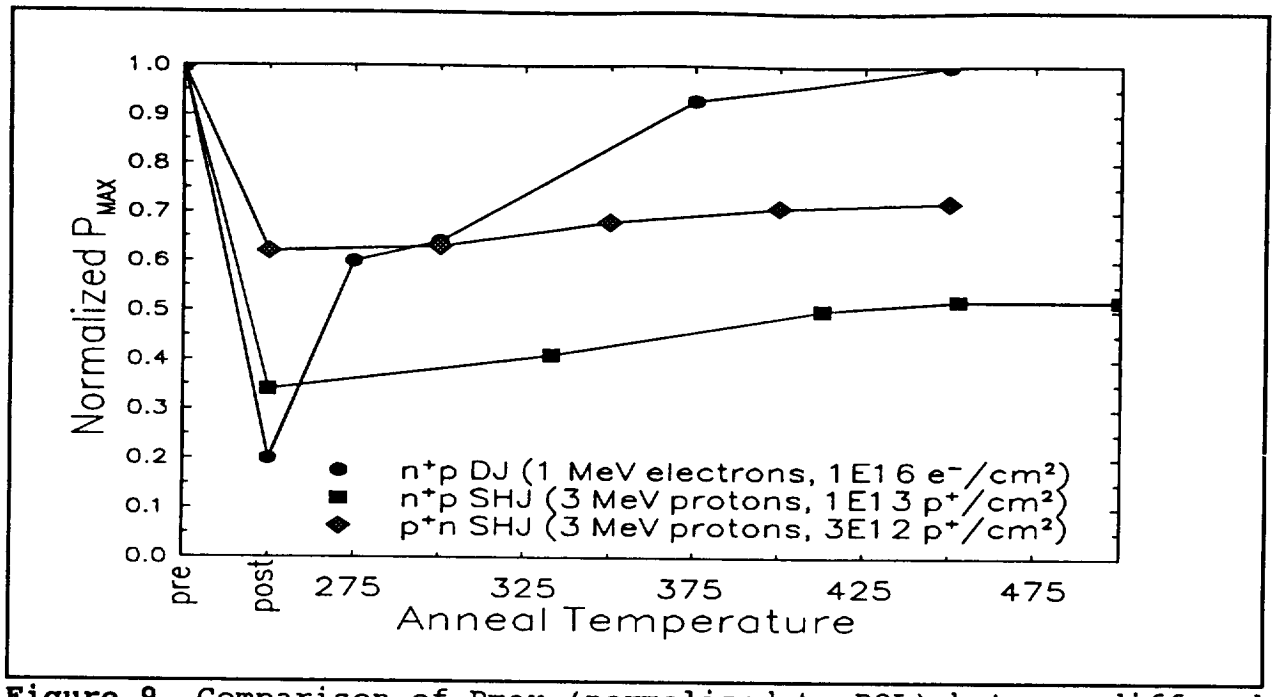

Figure 9 Comparison of Pmax (normalized to BOL) between diffused junctions (DJ), and both p-type and n-type MOCVD junctions. Pmax in the DJ cells recovered substantially while the MOCVD ones only recovered minimally.

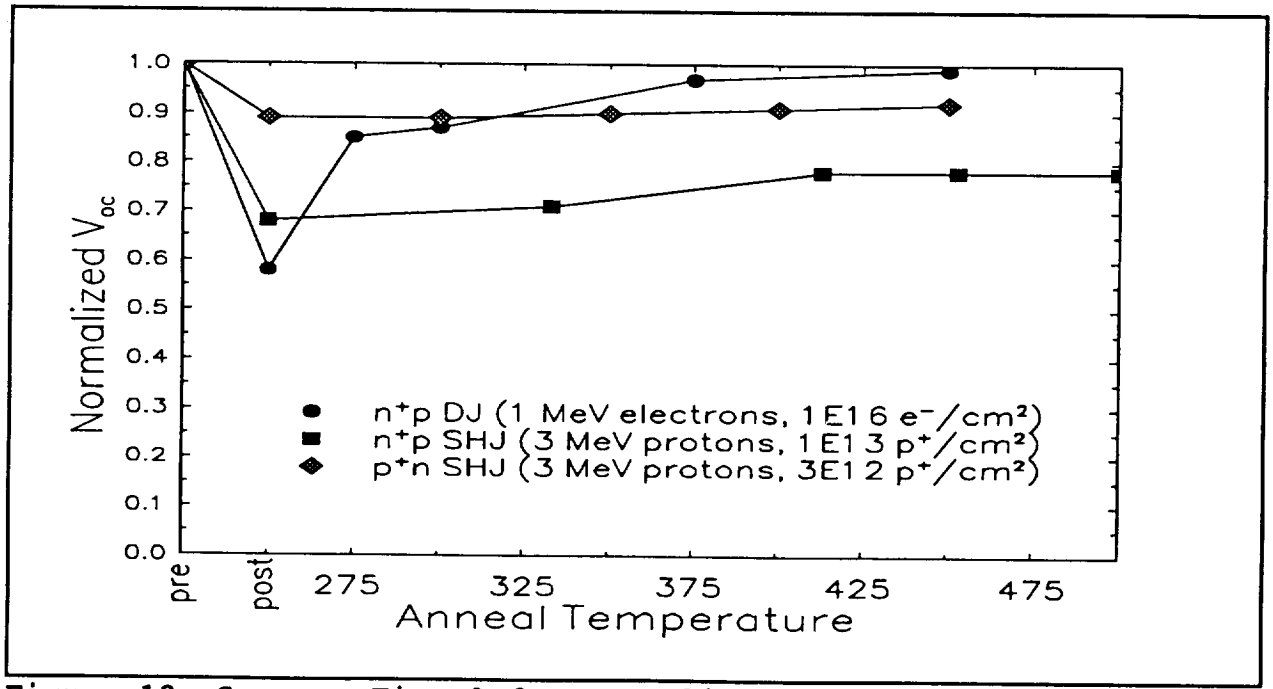

Figure 10 Same as Fig. 9 for normalized Voc. The same trend exists for Voc as for Pmax above.

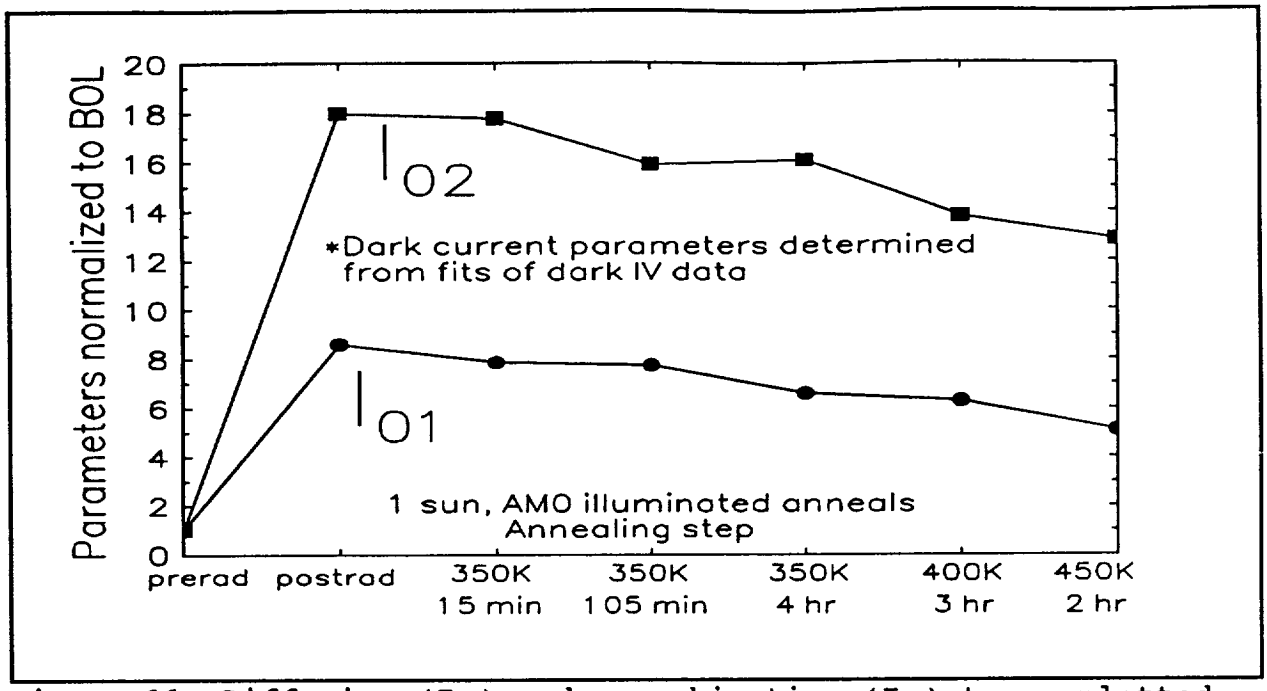

Figure 11 Diffusion (I_{01}) and recombination (I_{02}) terms plotted normalized to the BOL to show relative changes. The increase in I_{02} dominates, but both terms show a decrease under illumination.